Correction

EARTH, ATMOSPHERIC, AND PLANETARY SCIENCES

Correction for "Evidence for indigenous nitrogen in sedimentary and aeolian deposits from the *Curiosity* rover investigations at Gale crater, Mars," by Jennifer C. Stern, Brad Sutter, Caroline Freissinet, Rafael Navarro-González, Christopher P. McKay, P. Douglas Archer Jr., Arnaud Buch, Anna E. Brunner, Patrice Coll, Jennifer L. Eigenbrode, Alberto G. Fairen, Heather B. Franz, Daniel P. Glavin, Srishti Kashyap, Amy C. McAdam, Douglas W. Ming, Andrew Steele, Cyril Szopa, James J. Wray, F. Javier Martín-Torres, Maria-Paz Zorzano, Pamela G. Conrad, Paul R. Mahaffy, and the MSL Science Team, which appeared in issue 14, April 7, 2015, of *Proc Natl Acad Sci USA* (112:4245–4250; first published March 23, 2015; 10.1073/pnas.1420932112).

The authors note that the MSL Science Team group author list published incorrectly. The group author information in the *SI Appendix*, including the list of authors in the MSL Science Team as well as their affiliations, has been corrected.

CORRECTION

Evidence for indigenous nitrogen in sedimentary and aeolian deposits from the *Curiosity* rover investigations at Gale crater, Mars

Jennifer C. Stern[a,1], Brad Sutter[b], Caroline Freissinet[c], Rafael Navarro-González[d], Christopher P. McKay[e], P. Douglas Archer Jr.[b], Arnaud Buch[f], Anna E. Brunner[a,g], Patrice Coll[h], Jennifer L. Eigenbrode[a], Alberto G. Fairen[i,j], Heather B. Franz[a,k], Daniel P. Glavin[a], Srishti Kashyap[a,l], Amy C. McAdam[a], Douglas W. Ming[m], Andrew Steele[n], Cyril Szopa[o], James J. Wray[p], F. Javier Martín-Torres[q,r], Maria-Paz Zorzano[i], Pamela G. Conrad[a], Paul R. Mahaffy[a], and the MSL Science Team[s,2]

[a]Solar System Exploration Division, Goddard Space Flight Center, National Aeronautics and Space Administration, Greenbelt, MD 20771; [b]Jacobs Technology, Inc., Johnson Space Center, National Aeronautics and Space Administration, Houston, TX 77058; [c]NASA Postdoctoral Program, Goddard Space Flight Center, National Aeronautics and Space Administration, Greenbelt, MD 20771; [d]Instituto de Ciencias Nucleares, Universidad Nacional Autónoma de México, 04510 Mexico D.F., Mexico; [e]Exobiology Branch, Ames Research Center, National Aeronautics and Space Administration, Moffett Field, CA 94035; [f]Laboratoire de Genie de Procedes et Materiaux, Ecole Centrale Paris, 92295 Chatenay-Malabry, France; [g]School of Earth and Space Exploration, Arizona State University, Tempe, AZ 85281; [h]Laboratoire Interuniversitaire des Systèmes Atmosphériques, Université Paris-Est Créteil, Université Paris Diderot and CNRS, 94000 Créteil, France; [i]Centro de Astrobiologia, 28850 Torrejón de Ardoz, Madrid, Spain; [j]Department of Astronomy, Cornell University, Ithaca, NY 14853; [k]Center for Research and Exploration in Space Science and Technology, University of Maryland, College Park, MD 20742; [l]Department of Microbiology University of Massachusetts, Amherst, MA 01003; [m]Astromaterials Research and Exploration Science Directorate, Johnson Space Center, National Aeronautics and Space Administration, Houston, TX 77058; [n]Geophysical Laboratory, Carnegie Institution of Washington, Washington, DC 20015; [o]Laboratoire Atmosphères, Milieux et Observations Spatiales, Université Pierre et Marie Curie, Université Versailles Saint-Quentin and CNRS, 75005 Paris, France; [p]School of Earth and Atmospheric Sciences Georgia Institute of Technology, Atlanta, GA 30332; [q]Instituto Andaluz de Ciencias de la Tierra (Consejo Superior de Investigaciones Científicas–Universidad de Granada), 18100 Armilla, Granada, Spain; [r]Division of Space Technology, Department of Computer Science, Electrical and Space Engineering, Luleå University of Technology, S-981 28 Kiruna, Sweden; and [s]Jet Propulsion Laboratory, Pasadena, CA 91109

The Sample Analysis at Mars (SAM) investigation on the Mars Science Laboratory (MSL) *Curiosity* rover has detected oxidized nitrogen-bearing compounds during pyrolysis of scooped aeolian sediments and drilled sedimentary deposits within Gale crater. Total N concentrations ranged from 20 to 250 nmol N per sample. After subtraction of known N sources in SAM, our results support the equivalent of 110–300 ppm of nitrate in the Rocknest (RN) aeolian samples, and 70–260 and 330–1,100 ppm nitrate in John Klein (JK) and Cumberland (CB) mudstone deposits, respectively. Discovery of indigenous martian nitrogen in Mars surface materials has important implications for habitability and, specifically, for the potential evolution of a nitrogen cycle at some point in martian history. The detection of nitrate in both wind-drifted fines (RN) and in mudstone (JK, CB) is likely a result of N_2 fixation to nitrate generated by thermal shock from impact or volcanic plume lightning on ancient Mars. Fixed nitrogen could have facilitated the development of a primitive nitrogen cycle on the surface of ancient Mars, potentially providing a biochemically accessible source of nitrogen.

Mars | nitrogen | astrobiology | nitrates | *Curiosity*

Terrestrial life requires a fixed form of nitrogen for incorporation into biomolecules such as nucleobases and amino acids that serve as building blocks for DNA, RNA, and proteins. Nitrogen in the form of N_2 comprises ~2% of the martian atmosphere (1–3), but little is known about other possible N reservoirs on Mars, including those that may contain fixed forms of N (i.e., NH_3, NH_4^+, or NO_3^-) in the mantle, crust, and sediments. Although Mars currently has ~0.15 mbar N_2 in its atmosphere (1), estimates of the primordial N inventory of the martian atmosphere range from 3 to 300 mbar N_2 (ref. 4, and references therein). Loss of N to impact erosion and stripping by solar wind have greatly reduced the N content of the martian atmosphere over time, the latter process resulting in a $^{14}N/^{15}N$ ratio of N_2 on Mars of 173 ± 11 measured by Mars Science Laboratory (MSL) (5), in agreement with *Viking* lander measurements (2, 3), and reflecting an enrichment of the heavier isotope of ^{15}N due to preferential escape of ^{14}N (6). This enrichment in the heavier stable isotope is consistent with the

behavior of other volatiles in Mars' atmosphere (1) and consistent with the estimated 50–90% loss of volatile species to space (7).

In addition to N_2 escape, the inventory of N on Mars must include potential N sequestration on the martian surface. Any N cycling on Mars requires breaking the N_2 triple bond through "fixation" via oxidation or reduction of atmospheric N_2. Nitrogen fixation on Earth is predominantly biological and occurs by conversion of N_2 to ammonia via enzyme-catalyzed reactions, although abiotic N_2 fixation also occurs at much lower levels, mostly by lightning and volcanism (e.g., ref. 8), and photolysis of marine organic N to NO_3^-, which has been hypothesized as a source of Atacama Desert NO_3^- (9). Several abiotic mechanisms have been proposed for N_2 fixation on Mars (10, 11) and subsequent incorporation of N into the sedimentary record (12, 13). The presence of N species in Mars surface sediments and shallow subsurface is predicted (e.g., ref. 14) and is additionally supported by the presence of

Significance

We present data supporting the presence of an indigenous source of fixed nitrogen on the surface of Mars in the form of nitrate. This fixed nitrogen may indicate the first stage in development of a primitive nitrogen cycle on the surface of ancient Mars and would have provided a biochemically accessible source of nitrogen.

nitrates in martian meteorites (15, 16), as well as other possible N phases (17, 18).

Assigning a martian source to any nitrogen measured by Sample Analysis at Mars (SAM) in samples from Gale crater (19, 20) requires rigorous analysis of N contributions from all possible sources, including terrestrial contamination from the SAM instrument itself, which we have done for this work. Here, we will (*i*) describe and quantify N species in scooped samples from an aeolian deposit and sedimentary materials from two drill sites in the Sheepbed mudstone as detected by SAM evolved gas analysis (EGA) and GCMS, (*ii*) evaluate and quantify the contributions of terrestrial N, and (*iii*) discuss possible N sources and implications of detection of martian N in Gale crater solid samples.

Methods

During SAM's nominal solid-sample analysis mode, EGA is performed, in which the quadrupole mass spectrometer (QMS) directly analyzes the gases released from samples heated from Mars ambient to ~870 °C at 35 °C/min under a ~0.8-sccm He flow and a pressure of ~25 mbar in the pyrolysis oven (21). Before analysis, a sieved (<150 μm) and portioned (<76 mm³) sample is delivered to the Sample Manipulation System and into one of SAM's quartz-glass cups, which has been preconditioned before the experiment by heating to >800 °C under a flow of He and active pumping by SAM's wide-range pumps. Gases evolved during pyrolysis are continuously monitored using the QMS, and a portion of the gases are sent to the hydrocarbon trap (Tenax) and then to the GCMS. The SAM instrument has been described in detail elsewhere (21, 22), and individual experimental parameters are presented in *SI Text*.

Data are presented for the three solid sample sites analyzed by SAM—Rocknest (RN), John Klein (JK), and Cumberland (CB). RN is an aeolian deposit consisting of fine-grained material with a bulk composition similar to martian fines previously characterized at other locations on Mars, and as such, the RN deposit is thought to be representative of both local soil and global dust on Mars (23, 24). JK and CB are both drilled samples from mudstone taken ~1.5 m from one another, and part of the Sheepbed member of the Yellowknife Bay formation in Gale crater. These deposits are inferred to be ancient fluvio-lacustrine deposits (25), and their mineralogy (26) suggests an ancient habitable environment at this location on Mars, as well as the possibility of indigenous organic carbon preserved in this mudstone (20). Although RN contains some component of globally distributed martian dust, the JK and CB locations, drilled ~3 m apart, represent a restricted time interval on a local scale, with a K-Ar age of 4.21 ± 0.35 billion years measured for these mudstones (27). Based on ground tests and models, the mass of the portion delivered to SAM was estimated to be 50 ± 8 mg (2σ SD) for the RN analyses (28), 45 ± 18 mg for the single portions at JK and CB, and 135 ± 31 mg for the triple portions at JK and CB (20). Multiple portions of the same sample from each site were analyzed.

Results

SAM Experiments on Mars. EGA (Fig. 1) and GCMS (Fig. 2) detected N-containing compounds including nitric oxide (NO) (base peak *m/z* 30), hydrogen cyanide (HCN) (base peak *m/z* 27), and trifluoro-*N*-methyl-acetamide (TFMA) (diagnostic peak *m/z* 127). Abundances are shown in Table 1, and mass spectra for each compound are shown in *SI Text*. Fig. 2 shows two reconstructed GC chromatograms from the CB-5 sample with *m/z* corresponding to the base peaks for each species (solid lines) compared with CB-6–residue, which can be considered a blank for CB-5 (dotted lines). TFMA is a compound produced when *N*-methyl-*N*-*tert*-butyldimethylsilyl-trifluoroacetamide (MTBSTFA) reacts with molecules containing labile hydrogen atoms, such as water. MTBSTFA, carried for one of SAM's wet chemistry experiments, is a terrestrial N-containing compound in SAM that contributes to the background (29, 30). Cyanogen chloride (ClCN) (base peak *m/z* 61) and tri-fluoroacetonitrile (TFA) (base peak *m/z* 69) were also identified at low abundance (~2–3 nmol) in GC chromatograms. The *m/z* 27 peak was identified as hydrogen cyanide (HCN) by matching *m/z* ratios of 26/27 from the National Institute of Standards and Technology database; however, definitive identification is complicated by mass interferences that can come from hydrocarbon fragments, and the HCN is poorly retained on the GC column. N_2 (*m/z* 28), N_2O (*m/z* 44), and NO_2 (*m/z* 46) could not be identified or quantified
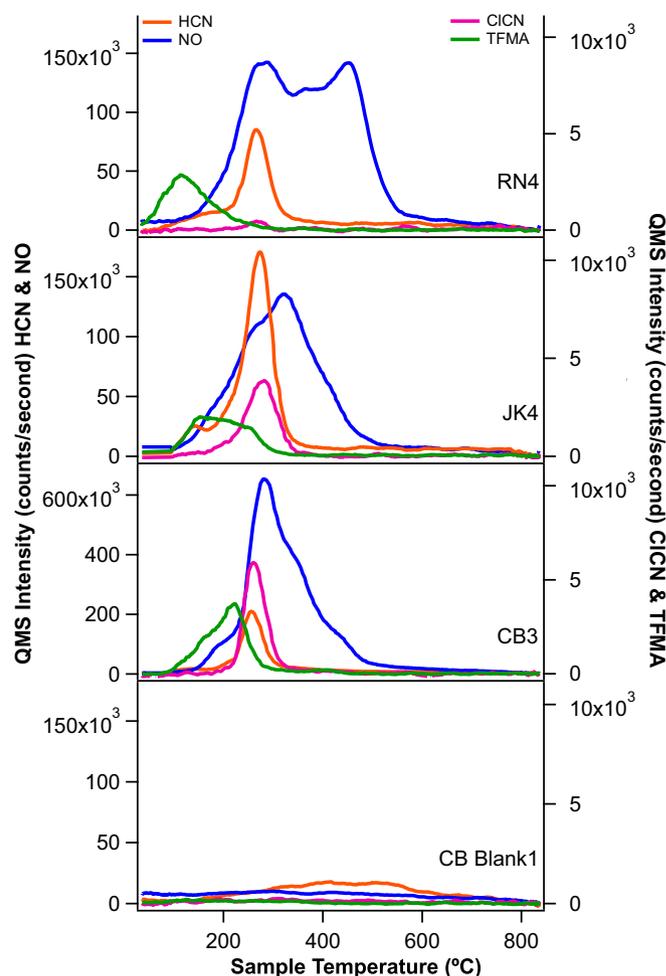

Fig. 1. Representative EGA pyrograms from RN, JK, and CB. Highest abundance species NO (blue) and HCN (orange) plotted as *m/z* 30 and 27, respectively, on left axis; low-abundance species ClCN (purple) and TFMA (green) plotted as *m/z* 61 and 127 on the right axis. Note the change in scale on the left axis for CB3, as NO was significantly more abundant in CB samples than at either RN or JK.

due to mass spectral interferences with CO, CO_2, and $^{12}C^{18}O^{16}O$ (respectively) from other species also evolving during EGA.

The reduced N species TFMA, ClCN, TFA, and HCN were detected at all sites (Fig. 1). All reduced species evolve at low temperature and peak before 300 °C. Generally, HCN is two times more abundant at JK and CB than at RN. HCN is present in all experiments above blank levels except for in CB-1. ClCN and TFA coevolve with HCN in all experiments in small amounts (2–3 nmol) but are more abundant at JK and CB than RN, where both are only present at subnanomole levels (Table 1).

The most abundant and variable species across the three samples is NO (Table 1 and Fig. 1), which generally evolves coincident with the onset of the oxygen release associated with thermal decomposition of chlorinated oxidants (20, 29). The average abundance of NO in RN1-4 is 212 ± 46 nmol and the release can be deconvolved into at least three NO evolutions: (*i*) a broad peak starting at 150 °C, centered at ~275 °C; (*ii*) a similarly broad release between 300 and 400 °C overlapping with the first release; and (*iii*) a sharper peak centered at ~475 °C. For JK, NO evolves in three major peaks centered at ~250, 300, and 400 °C, with total NO abundance similar to RN (JK single portion average of 202 ± 43 nmol). Unlike RN, there was no large evolution of NO >400 °C at JK or CB. CB shows the highest NO abundances of 462 ± 62 nmol
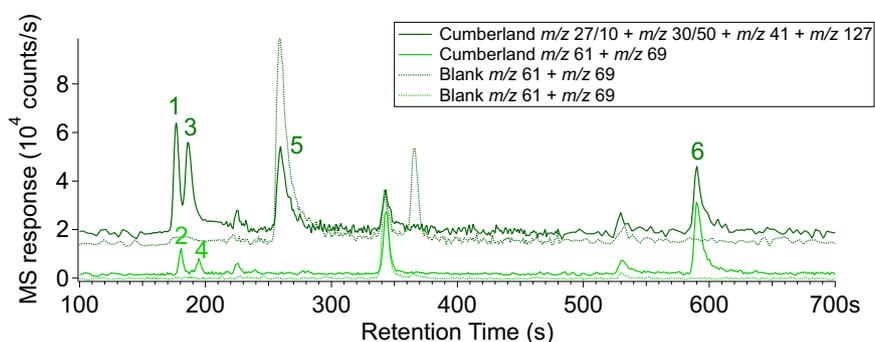
Fig. 2. GC chromatograms of CB-5 sample with *m/z* corresponding to the base or diagnostic peak of each of the N-bearing compounds identified. 1, NO (*m/z* 30); 2, TFA (*m/z* 69); 3, HCN (*m/z* 27); 4, ClCN (*m/z* 61); 5, CH$_3$CN (*m/z* 41); 6, TFMA (*m/z* 127). Division factors were applied to the most abundant compounds for scaling: factor 10 for *m/z* 27 and factor 50 for *m/z* 30. None of the chosen masses contribute to another N-bearing compound identified in each chromatogram. Because of partial coelutions between the first four GC peaks, two separate chromatograms were reconstructed (dark green and light green plain lines). The corresponding dotted lines are the reconstructed chromatograms of the reheated CB-6–residue sample, which has the same GC temperature cut as CB-5 and can thus be considered as a blank. Although acetonitrile (CH$_3$CN) (*m/z* 41) is detected in the GC, its detection in EGA is complicated by methylpropene, which constitutes the majority of the signal at *m/z* 41.

for the average of CB single portions. The NO evolution from CB starts <200 °C, just before the onset of oxygen, followed by large peak at (275 °C) with shoulders at 350 and 425 °C (Fig. 1.)

Blanks and Instrument Background. The terrestrial derivatization reagent MTBSTFA contributed to the SAM background in both the blanks and in samples (29, 30). Masses associated with all of the N compounds detected by SAM EGA are also detected in laboratory experiments performing EGA on fused silica doped with MTBSTFA and 1 wt % perchlorate (*SI Text*). MTBSTFA has one N atom and is therefore a potential source of N that could

react with other species from the sample. Therefore, terrestrial N sources must be quantified to verify that the N detected is martian. The method to quantify MTBSTFA-derived nitrogen is modified from the method to quantify MTBSTFA-derived carbon from Ming et al. (20) and is detailed in *SI Text*. Estimates for MTSBTFA-derived N are compared with total detected N and used to adjust NO abundances (Table 1).

Discussion

Constraining MTBSFTA Sources of N. Total N detected in SAM EGA is more abundant than N estimates from MTBSTFA contributions

Table 1. Abundances of N compounds at RN, JK, and CB

Sample	Total detected N, nmol	HCN, nmol	NO, nmol	ClCN, nmol	TFA, nmol	TFMA, nmol	MTBSTFA-derived N, nmol*	Residual N, nmol†	Maximum % NO from MTBSTFA, %	Corrected NO, nmol‡
RN-Blank	15 ± 3	2.5 ± 0.5	12 ± 2	ND	ND	<1	49 ± 10	46 ± 9	100	NA
RN-1	215 ± 43	28 ± 6	186 ± 37	ND	ND	<1	54 ± 11	50 ± 10	27 ± 8	135 ± 27
RN-2	321 ± 64	40 ± 8	280 ± 56	ND	ND	1.3 ± 0.3	79 ± 16	76 ± 15	27 ± 8	204 ± 41
RN-3	231 ± 46	26 ± 5	201 ± 41	<1	<1	1.9 ± 0.4	70 ± 14	67 ± 13	33 ± 9	136 ± 27
RN-4	211 ± 42	25 ± 5	180 ± 36	<1	<1	5.0 ± 1.0	79 ± 16	75 ± 15	42 ± 12	104 ± 21
JK-Blank	30 ± 6	1.1 ± 0.2	26 ± 5	ND	2.1 ± 0.4	1.5 ± 0.3	86 ± 17	84 ± 17	100	NA
JK-1	291 ± 58	53 ± 11	230 ± 46	2.1 ± 0.4	1.5 ± 0.3	4.1 ± 0.8	127 ± 25	124 ± 25	54 ± 15	106 ± 21
JK-2	277 ± 55	46 ± 9	223 ± 45	2.9 ± 0.6	1.5 ± 0.3	3.9 ± 0.8	118 ± 24	115 ± 23	52 ± 15	108 ± 22
JK-3 (3× portion)	680 ± 136	83 ± 17	579 ± 116	2.0 ± 0.4	4.2 ± 0.8	11 ± 2	223 ± 45	221 ± 44	38 ± 11	359 ± 72
JK-4	213 ± 43	54 ± 11	152 ± 31	1.7 ± 0.3	1.8 ± 0.4	3.5 ± 0.7	80 ± 16	78 ± 16	51 ± 14	75 ± 15
CB-Blank1	90 ± 18	24 ± 5	62 ± 13	<1	ND	3.1 ± 0.6	116 ± 23	88 ± 18	100	NA
CB-1	272 ± 54	15 ± 3	246 ± 49	1.4 ± 0.3	2.7 ± 0.5	6.9 ± 1.4	99 ± 20	71 ± 14	29 ± 8	175 ± 35
CB-2	447 ± 89	47 ± 10	391 ± 78	1.6 ± 0.3	3.5 ± 0.7	3.7 ± 0.7	85 ± 17	57 ± 11	15 ± 4	334 ± 67
CB-3	551 ± 110	48 ± 10	494 ± 99	2.3 ± 0.5	2.6 ± 0.5	4.5 ± 0.9	68 ± 14	40 ± 8	8 ± 2	454 ± 91
CB-5	560 ± 112	53 ± 11	502 ± 100	2.7 ± 0.5	<1	2.0 ± 0.4	41 ± 8	13 ± 3	3 ± 1	490 ± 98
CB-6 (3× portion)§	466 ± 93	16 ± 3	448 ± 90	<1	1.2 ± 0.3	<1	35 ± 7	6 ± 1	~1	443 ± 89
CB-6 (residue)	88 ± 18	25 ± 5	60 ± 12	ND	<1	2.7 ± 0.5	81 ± 16	52 ± 10	86 ± 24	NA
CB-7 (3× portion)§	357 ± 71	11 ± 2	340 ± 68	2.0 ± 0.4	2.8 ± 0.6	<1	43 ± 9	13 ± 3	4 ± 1	327 ± 65
CB-Blank2	25 ± 5	ND	25 ± 5	ND	ND	ND	25 ± 5	25 ± 5	100	NA

Contributions of N from MTBSTFA can be used to correct for the maximum terrestrial contribution of N to NO in a worst-case scenario assumption that all MTBSTFA-N forms NO.

*Total MTBSTFA-derived N in nanomoles determined from the sum of the EGA-QMS quantification of abundances of silylated products. See *SI Text* for details.

†Residual N is the N in nanomoles resulting from subtraction of reduced N species detected in the blank for each set of experiments (RN-Blank, 2.7 ± 0.5 nmol; JK-Blank, 4.7 ± 0.9 nmol; CB-Blank1, 28 ± 6 nmol). This reduced N is assumed to be derived from MTBSTFA.

‡Corrected NO is derived by subtracting the nanomoles of residual N from the nanomoles of NO to take into account MTBSTFA-derived N.

§In CB-6 and -7, three portions of sample were deposited into a hot cup (~250 °C), driving off a significant amount of all N species before the sample analysis. The calculated abundances of N-bearing species are included for completeness but are expected to differ from previous CB runs because of the way the samples were handled before analysis (Table 1 and *SI Text*).
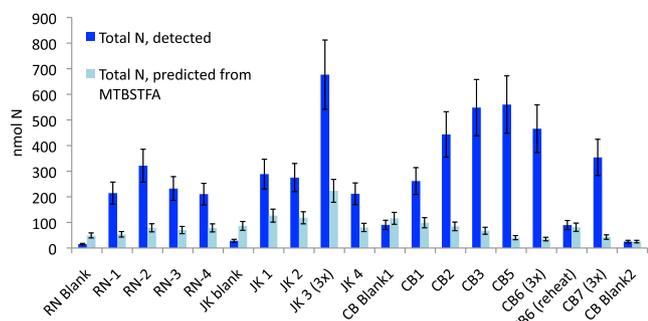
Fig. 3. The total nanomoles of N in the sum of all N species detected (NO, HCN, ClCN, TFA, TFMA; Table 1) in blue, compared with the worst-case scenario prediction of nanomoles of N contributed by MTBSTFA (Table 1 and *SI Text*) in light blue. In blanks, except for CB-Blank2, the estimate of MTBSTFA-derived N is greater than actual N detected. CB samples had the largest abundance of detected N species, and the lowest percentage N contribution from MTBSTFA (Table 1).

(Table 1 and Fig. 3). Estimated MTBSTFA contribution to N for RN, JK, and CB blanks is larger than the actual amount of N detected in any of these blanks (Table 1). This "missing N" may simply be attributed to the high likelihood that our worst-case scenario calculations of MTBSTFA-derived N are overestimates.

It is difficult from laboratory experiments to determine the MTBSTFA-N contribution to individual N species detected in martian samples. An experiment reheating sample CB-6 after reexposure to the sample carousel, where the sample would have been in contact with MTBSTFA vapor, suggests that reduced species are predominantly MTBSTFA derived, but that NO is produced by thermal decomposition of martian sediments. This is further supported by the consistent evolution temperature of HCN (and ClCN) in RN, JK, and CB EGA pyrograms (Fig. 1), whereas there is considerable variation in the NO release profile across the three sites.

Nevertheless, to demonstrate the strength of the evidence for a martian NO source in these samples, we assume a worst-case scenario in which all MTBSTFA-derived N (minus reduced species present in SAM experimental blanks) is combusted to NO, even though laboratory experiments indicate that reduced species HCN, TFMA, TFA, and ClCN are also formed, and our CB-6 reheat experiment supports an MTBSTFA source for these reduced species. Based on our calculations, MTBSTFA contributed 27–42% of the NO at RN, 38–54% at JK, and 1–29% at CB (Table 1). If we take a slightly less conservative but more realistic approach and assume that the reduced species observed are predominantly products of MTBSTFA decomposition, then MTBSTFA contributed 13–27% of the NO at RN, 14–30% at JK, and 1–10% at CB.

N-Bearing Species Distribution. NO is the dominant N-bearing species in the RN, JK, and CB samples, and is more abundant than our estimates for total MTBSTFA-derived N. The main source of NO in these samples has been suggested to be thermal decomposition of nitrates present in the samples (31). Thermal decomposition of nitrates is possible at the temperatures observed in SAM EGA data (decomposition begins at <200 °C), particularly if iron nitrates are present (32). Alkali (e.g., Na, K) and alkaline earth (e.g., Mg, Ca) metal nitrates generally decompose into nitric oxide at elevated temperatures (>560 °C); however, their decomposition temperatures can decrease in the presence of perchlorates and metal oxides (31, 33). Alternative or additional sources of NO include combustion of labile organic nitrogen-bearing compounds (other than MTBSTFA) under oxidizing conditions (34). However, this would represent a large amount of organic N, and as no organic compounds of martian origin have been definitively identified, an inorganic source of N is the more plausible origin for the NO.

Additional laboratory experiments to characterize the thermal decomposition temperatures of calcium nitrate tetrahydrate [$Ca(NO_3)_2 \cdot 4H_2O$; Sigma], iron(III) nitrate nonahydrate [$Fe(NO_3)_3 \cdot 9H_2O$; Sigma], and magnesium nitrate hexahydrate [$Mg(NO_3)_2 \cdot 6H_2O$; Sigma] for comparison with SAM EGA data were performed using a custom-built SAM-like laboratory system (*SI Text*). Onset of *m/z* 30 evolution of each species can be diagnostic of the source of NO in martian solid samples: ~100 °C for $Fe(NO_3)_3$, ~300 °C for $Mg(NO_3)_2$, and ~500 °C for $Ca(NO_3)_2$. Both JK and CB have their primary peak maximums ~300 °C, whereas the release profile at RN includes a peak maximum ~300 °C as well as a second one ~450 °C, consistent with the double peak release shown by $Fe(NO_3)_3$ (Fig. 4). The two-step decomposition of $Fe(NO_3)_3$ has been noted in the literature (32) and is characterized by a lower temperature release occurring over a broad temperature range, followed by a second, sharper release over a narrower range of temperature. This two-step release is thought to be a result of dehydration accompanied by hydrolysis, in which iron nitrate melts in its own water of crystallization followed by the evaporation and precipitation of $Fe(OH)NO_3$, ultimately resulting in the formation of Fe_2O_3 as the final product.

Although HCN is generally present at higher abundances in samples than in blanks, at present it is difficult to assign a nonterrestrial origin to this compound. However, it is not unreasonable to assume that pyrolysis of martian surface materials may produce HCN from macromolecular material of meteoritic, cometary, and interplanetary dust particle origin (35, 36).

Significance of Results. Detection of indigenous, fixed N in martian rocks and sediments has significant implications for the past habitability potential of Mars, as life on Earth requires bioavailability of N for synthesis of key biomolecules. Several hypotheses exist for mechanisms of cycling of N on Mars and these depend upon breaking the N_2 triple bond through "fixation" or reduction of atmospheric N_2. Detection of NO formed from products of O_2, CO_2, and N_2 photodissociation in the martian thermosphere by *Mars Express* was reported in 2005 (37). This suggests that N is currently being fixed in the martian thermosphere, although it is unknown how much, if any, is transported to the lower atmosphere and surface. Thermal shock, either from lightning or impact, has been the favored mechanism by which the N_2 bond could have been broken in the early martian (and terrestrial) atmosphere, resulting in HNO^-, which reacts to form NO_2^- and NO_3^- in the presence of liquid water (4, 12, 38, 39). If NO detected by SAM EGA is attributable to the decomposition of nitrates, as laboratory
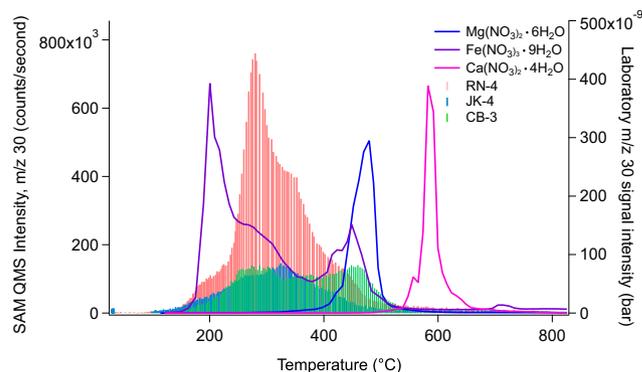
Fig. 4. The *m/z* 30 trace for EGA of three nitrate species, calcium nitrate tetrahydrate [$Ca(NO_3)_2 \cdot 4H_2O$], iron(III) nitrate nonahydrate [$Fe(NO_3)_3 \cdot 9H_2O$], and magnesium nitrate hexahydrate [$Mg(NO_3)_2 \cdot 6H_2O$] run on a laboratory SAM-like system compared with RN, JK, and CB SAM experiments. The release profile at RN-4 is most consistent with the two-step decomposition of $Fe(NO_3)_3$, suggesting that Fe-nitrate may be a component of the RN sample.

experiments suggest, this would imply that (*i*) N fixation has occurred on Mars, and (*ii*) a biochemically available source of N is present on Mars and likely was in the past.

Based on estimates of sample mass and corrections for terrestrial N contribution, nitrogen present as NO in Gale crater is equivalent to 20–250 ppm N, with the highest concentrations in the CB mudstone. Converted to the equivalent amount of nitrate, this gives 110–300 ppm of nitrate in the RN aeolian samples, 70–260 ppm nitrate in JK mudstone samples, and 330–1,100 ppm nitrate in CB mudstone samples. Manning et al. (40) calculated an impact generated nitrate reservoir of $\sim 5 \times 10^{15}$ mol on Mars that is unlikely to have experienced significant decomposition. This translates into ~ 0.11 wt % NO_3, using a 950-m impact veneer depth (e.g., ref. 40) and a soil density of 2 g/cm^3, and is consistent with the upper limit of our detection of ~ 0.11 wt % NO_3 at CB. Our detections also fall within the estimates of nitrate concentration from meteorites, which vary widely from recent detection of $4,800 \pm 60$ ppm nitrate in the martian meteorite EETA79001 (15) to previous estimates of >1 ppm (16).

The detection of nitrate at one site representing the martian global dust/local soil reservoir and two representing a potential relict lakebed (25) may suggest widespread atmospheric deposition. The hyperarid Atacama Desert provides a terrestrial analog for abiotic N fixation and deposition, as biological inputs are severely limited, and oxidized N is stored in soils as nitrate instead of being removed via denitrification or leaching by water (9). Understanding whether similar processes are currently fixing N_2 to NO_3 and subsequently depositing nitrate on the martian surface is compelling for the habitability of Mars in the present and recent past. The abundances detected in all three Mars samples (~ 0.01–0.1 wt % NO_3) are an order of magnitude lower than those in the Atacama Desert and Dry Valleys of Antarctica, which range from ~ 0.1 to >1 wt % NO_3 (e.g., ref. 41) and can be as high as 36% in Atacama Desert nitrate ore deposits (42). The low nitrate abundance in martian samples is consistent with models of the impact-generated nitrate reservoir (e.g., ref. 40), suggesting that we are detecting the products of ancient N-fixation processes under different atmospheric conditions, with no additional inputs, and negligible decomposition of the original reservoir. The difference in abundance between JK mudstone (0.01–0.03 wt % NO_3) and CB mudstone (up to ~ 0.1 wt % NO_3), two mudstone samples taken ~ 1.5 m apart, could reflect postdepositional leaching of NO_3 from JK, which shows evidence of more alteration than CB (26). Alternatively, increased nitrate abundance at CB could reflect additional past input via some in situ fixation mechanism, biological or

not. Detection of indigenous reduced N (e.g., ammonia) would support biological fixation; however, not only is ammonia difficult to detect by SAM (*SI Text*), but it is readily destroyed by photochemistry, and thus not likely to have been preserved unless structurally incorporated into minerals. One interpretation for the persistence of oxidized N and the apparent lack of reduced N in a lacustrine environment is the absence of development of chemistry to return N into the atmosphere [on Earth, the biological process of denitrification (43)]. Thus, despite the fact that these ancient aqueous environments represented by Yellowknife Bay sediments on Mars once had a high potential for habitability (25), our analysis of these sediments does not support the presence of a complex N cycle analogous to that which drives life on Earth.

Conclusion

Nitrogen species were detected in pyrolysis of one sample scooped from an aeolian deposit and two samples drilled from the same sedimentary rock unit in Yellowknife Bay. The molar abundance of N in these samples exceeds that predicted to be present due to all known terrestrial instrument sources. The bulk of the N detected is in the form of nitric oxide (NO) and may indicate a mineralogical sink for atmospheric N_2 in the form of nitrate, with estimated abundance of up to $\sim 1,100$ ppm NO_3^- in martian sedimentary deposits. The detection of NO in both wind-drifted fines (RN) and in mudstone (JK, CB) likely reflects ancient impact and/or volcanic plume lightning generated N_2 fixation to NO_3 (10–12). Fixed N is essential to terrestrial life, and this requirement has driven the evolution of metabolism on Earth. The presence of fixed N on Mars suggests that, at some point, the first half of a nitrogen cycle was established. On Earth, N is cycled back into the atmosphere by denitrification via biological activity, but on Mars, the probable absence of near-surface life in post-Noachian times would result in fixed N accumulating as nitrate in the martian geologic record. Nevertheless, if pre-Noachian life had arisen on Mars, it is reasonable to assume that it exploited the available nitrate, and our results suggest that the search for stratigraphic evidence of an ancient martian N cycle should continue.

1. Mahaffy PR, et al.; MSL Science Team (2013) Abundance and isotopic composition of gases in the martian atmosphere from the *Curiosity* rover. *Science* 341(6143):263–266.
2. Nier A, McElroy MB (1977) Composition and structure of Mars' upper atmosphere: Results from the neutral mass spectrometers on Viking 1 and 2. *J Geophys Res* 82(28):4341–4349.
3. Owen T, et al. (1977) The composition of the atmosphere at the surface of Mars. *J Geophys Res* 82(28):4635–4639.
4. McKay CP, Stoker CR (1989) The early environment and its evolution on Mars: Implication for life. *Rev Geophys* 27(2):189–214.
5. Wong MH, et al. (2013) Isotopes of nitrogen on Mars: Atmospheric measurements by *Curiosity*'s mass spectrometer. *Geophys Res Lett* 40(23):6033–6037.
6. Jakosky BM, Pepin RO, Johnson RE, Fox JL (1994) Mars atmospheric loss and isotopic fractionation by solar-wind-induced sputtering and photochemical escape. *Icarus* 111(2):271–288.
7. Jakosky BM, Phillips RJ (2001) Mars' volatile and climate history. *Nature* 412(6843):237–244.
8. Oyarzun J, Oyarzun R (2007) Massive volcanism in the Altiplano-Puna Volcanic Plateau and formation of the huge Atacama Desert nitrate deposits: A case for thermal and electric fixation of atmospheric nitrogen. *Int Geol Rev* 49(10):962–968.
9. Ewing SA, et al. (2007) Rainfall limit of the N cycle on Earth. *Global Biogeochem Cycles* 21(3):1–12.
10. Segura A, Navarro-González R (2005) Nitrogen fixation on early Mars by volcanic lightning and other sources. *Geophys Res Lett* 32(5):L05203.
11. Summers DP, Khare B (2007) Nitrogen fixation on early Mars and other terrestrial planets: Experimental demonstration of abiotic fixation reactions to nitrite and nitrate. *Astrobiology* 7(2):333–341.
12. Mancinelli RL, McKay CP (1988) The evolution of nitrogen cycling. *Orig Life Evol Biosph* 18(4):311–325.
13. Summers DP, Chang S (1993) Prebiotic ammonia from reduction of nitrite by iron (II) on the early Earth. *Nature* 365:630–633.
14. Manning CV, McKay CP, Zahnle KJ (2008) The nitrogen cycle on Mars: Impact decomposition of near-surface nitrates as a source for a nitrogen steady state. *Icarus* 197(1):60–64.
15. Kounaves SP, Carrier BL, O'Neil GD, Stroble ST, Claire MW (2014) Evidence of martian perchlorate, chlorate, and nitrate in Mars meteorite EETA79001: Implications for oxidants and organics. *Icarus* 229:206–213.
16. Grady M, Wright I, Pillinger C (1995) A search for nitrates in Martian meteorites. *J Geophys Res Planets* 100(E3):5449–5455.
17. Fogel ML, Steele A (2013) Nitrogen in extraterrestrial environments: Clues to the possible presence of life. *Elements* 9(5):367–372.
18. Aoudjehane HC, et al. (2012) Tissint martian meteorite: A fresh look at the interior, surface, and atmosphere of Mars. *Science* 338(6108):785–788.
19. Archer PD, et al. (2014) Abundances and implications of volatile-bearing species from evolved gas analysis of the Rocknest aeolian deposit, Gale crater, Mars. *J Geophys Res Planets* 119(1):237–254.
20. Ming DW, et al.; MSL Science Team (2014) Volatile and organic compositions of sedimentary rocks in Yellowknife Bay, Gale crater, Mars. *Science* 343(6169):1245267.
21. Mahaffy P, et al. (2012) The Sample Analysis at Mars investigation and instrument suite. *Space Sci Rev* 170(1-4):401–478.
22. Franz HB, et al. (2014) Analytical techniques for retrieval of atmospheric composition with the quadrupole mass spectrometer of the Sample Analysis at Mars instrument suite on Mars Science Laboratory. *Planet Space Sci* 96:99–113.
23. Bish DL, et al.; MSL Science Team (2013) X-ray diffraction results from Mars Science Laboratory: Mineralogy of Rocknest at Gale crater. *Science* 341(6153):1238932.

EARTH, ATMOSPHERIC, AND PLANETARY SCIENCES

24. Blake DF, et al.; MSL Science Team (2013) *Curiosity* at Gale crater, Mars: Characterization and analysis of the Rocknest sand shadow. *Science* 341(6153):1239505.

25. Grotzinger JP, et al.; MSL Science Team (2014) A habitable fluvio-lacustrine environment at Yellowknife Bay, Gale crater, Mars. *Science* 343(6169):1242777.

26. Vaniman DT, et al.; MSL Science Team (2014) Mineralogy of a mudstone at Yellowknife Bay, Gale crater, Mars. *Science* 343(6169):1243480.

27. Farley KA, et al.; MSL Science Team (2014) In situ radiometric and exposure age dating of the martian surface. *Science* 343(6169):1247166.

28. Anderson RC, et al. (2012) Collecting samples in Gale crater, Mars; an overview of the Mars Science Laboratory sample acquisition, sample processing and handling system. *Space Sci Rev* 170(1-4):57–75.

29. Glavin DP, et al. (2013) Evidence for perchlorates and the origin of chlorinated hydrocarbons detected by SAM at the Rocknest aeolian deposit in Gale crater. *J Geophys Res Planets* 118(10):1955–1973.

30. Leshin LA, et al.; MSL Science Team (2013) Volatile, isotope, and organic analysis of martian fines with the Mars *Curiosity* rover. *Science* 341(6153):1238937.

31. Navarro-González R, et al. (2013) Possible detection of nitrates on Mars by the Sample Analysis at Mars (SAM) instrument. *Lunar Planet Sci XLIV* (Lunar and Planetary Institute, Houston), 2648.

32. Wieczorek-Ciurowa K, Kozak A (1999) The thermal decomposition of Fe (NO3) 3•9H$_2$O. *J Therm Anal Calorim* 58(3):647–651.

33. Hoshino Y, Utsunomiya T, Abe O (1981) The thermal decomposition of sodium nitrate and the effects of several oxides on the decomposition. *Bull Chem Soc Jpn* 54(5):1385–1391.

34. Navarro-González R, Iñiguez E, de la Rosa J, McKay CP (2009) Characterization of organics, microorganisms, desert soils, and Mars-like soils by thermal volatilization coupled to mass spectrometry and their implications for the search for organics on Mars by Phoenix and future space missions. *Astrobiology* 9(8):703–715.

35. Ehrenfreund P, Charnley SB (2000) Organic molecules in the interstellar medium, comets, and meteorites: A voyage from dark clouds to the early Earth. *Annu Rev Astron Astrophys* 38(1):427–483.

36. Sephton MA (2012) Pyrolysis and mass spectrometry studies of meteoritic organic matter. *Mass Spectrom Rev* 31(5):560–569.

37. Bertaux J-L, et al.; SPICAM Team (2005) Nightglow in the upper atmosphere of Mars and implications for atmospheric transport. *Science* 307(5709):566–569.

38. Mancinelli RL (1996) The search for nitrogen compounds on the surface of Mars. *Adv Space Res* 18(12):241–248.

39. Navarro-González R, Molina MJ, Molina LT (1998) Nitrogen fixation by volcanic lightning in the early Earth. *Geophys Res Lett* 25(16):3123–3126.

40. Manning CV, Zahnle KJ, McKay CP (2009) Impact processing of nitrogen on early Mars. *Icarus* 199(2):273–285.

41. Kounaves SP, et al. (2010) Discovery of natural perchlorate in the Antarctic Dry Valleys and its global implications. *Environ Sci Technol* 44(7):2360–2364.

42. Ericksen GE (1983) The Chilean nitrate deposits. *Am Sci* 71:366–374.

43. Capone DG, Popa R, Flood B, Nealson KH (2006) Geochemistry. Follow the nitrogen. *Science* 312(5774):708–709.